Supplementary Information

Three-dimensional stretchable microelectronics by projection micro stereolithography (PµSL)

Yuejiao Wang,[1,2] Xiang Li, [2,3] Sufeng Fan,[1,2] Xiaobin Feng,[1,2] Ke Cao,[4] Qi Ge,[5*] Libo Gao,[4*] Yang Lu[1,2,3*]

1 Department of Mechanical Engineering, City University of Hong Kong, Kowloon, Hong Kong SAR, China

2 Nanomanufacturing Laboratory (NML), City University of Hong Kong Shenzhen Research Institute, Shenzhen 518057, China

3 CityU-Xidian Joint Laboratory of Micro/Nano-Manufacturing, Shenzhen 518057, China

4 School of Mechano-Electronic Engineering, Xidian University, Xian 710071, China

5 Department of Mechanical and Energy Engineering, Southern University of Science and Technology, Shenzhen 518055, China

* Author to whom correspondence should be addressed:

Email: geq@sustech.edu.cn; lbgao@xidian.edu.cn; yanglu@cityu.edu.hk

Supplementary Text

1. Finite element analyses of three different 3D structure designs

U-shaped structure contains semicircles connected by vertical lines whereas horseshoe-shaped structure is made up of an arc jointed to its vertical-flipped counterpart. The geometrical parameters of these three designs including thickness (t), width (w), height (a), and wavelength (λ) (Figure S1a) are kept the same for comparison. Specially, to allow three 3D structures to have a good attachment on substrate, short line segments ($l = \sim 0.07\lambda$) are added on the bottom to connect unit cells.

Due to bending-dominated deformation, higher values of tensile/compressive strains all occur at the surface for all three structures, but well below the failure strain of the polymer materials (~5%, see Figure S2d). As shown in Figure 2a, tensile loading of the sinusoidal structures causes sharp stress concentrations at the lower surface of the top region. By contrast, although both U-shaped and horseshoe-shaped design also possess the maximum strain at the same location, it is broader distributed and comparable high values can be found as well at the corresponding upper surface and the regions next to bottom line segments (Figure 2b, c). In conclusion, the horseshoe-shaped design outperforms the other two by reducing the maximum strain of sinusoidal design by 53% and U-shaped design by 13%, showing the strongest ability to accommodate large stretching strains. Meanwhile, the three structures are also able to bear axial compression deformation (20%, Figure S2(a-c)), under which horseshoe-shaped structure is still the optimal design among others despite the smaller difference than being stretched.

2. Stretchability analyses of horseshoe-shaped structure

To further explore the relationship between stretchability and geometrical parameters of 3D horseshoe-shaped structure including arc angle (θ), radius (R), and width (w) (Figure S1a), we adopted the analytical model from the work by Widlund et al [1]. Note

that the additional line segment parts are not considered in this model, which is different from the finite element analysis. The stretchability of different designs is evaluated by $\varepsilon_{max}/\varepsilon_{app}$, where ε_{max} is the maximum strain on the structure under the applied overall uniaxial strain ε_{app}, since smaller $\varepsilon_{max}/\varepsilon_{app}$ represents greater stretchability based on failure criterion of ε_{max} reaching the intrinsic failure strain of the materials. Building on the Winkler curved beam (CB) theories, $\varepsilon_{max}/\varepsilon_{app}$ of serpentine-shaped ribbons is deduced as

$$\frac{\varepsilon_{max}}{\varepsilon_{app}} =$$

$$\frac{\frac{w}{R}\left[\frac{12}{2-\frac{w}{R}}+\left(\frac{12}{2-\frac{w}{R}}-\frac{w}{R}\right)\left(sin\theta+\frac{L}{2R}cos\theta\right)\right]\left(cos\theta-\frac{L}{2R}sin\theta\right)}{cos^2\theta\left[\frac{L^3}{2R^3}+3\left(\frac{\pi}{2}+\theta\right)\frac{L^2}{R^2}+12\frac{L}{R}-12\left(\frac{\pi}{2}+\theta\right)\right]+sin2\theta\left[6\left(\frac{\pi}{2}+\theta\right)\frac{L}{R}+9\right)\right]+\frac{w^2}{Rt}\left[\left(\frac{\pi}{2}+\theta\right)\left(\frac{L}{2R}cos\theta+sin\theta\right)^2+\frac{L}{2R}\left(sin\theta+\frac{2E}{2G}cos\theta\right)\right]+18\left(\frac{\pi}{2}+\theta\right)}$$

(1) [1].

Where the geometrical parameters parameter L is taken as zero for our horseshoe-shaped structure. Since t almost has no impact on $\varepsilon_{max}/\varepsilon_{app}$, we assume $t/w=1$. Thus, the equation is simplified as

$$\frac{\varepsilon_{max}}{\varepsilon_{app}} = g\left(\frac{w}{R},\theta\right) = \frac{\frac{w}{R}cos\theta\left[\frac{12}{2-\frac{w}{R}}+\left(\frac{12}{2-\frac{w}{R}}-\frac{w}{R}\right)sin\theta\right]}{cos^2\theta\left[-12\left(\frac{\pi}{2}+\theta\right)\right]+9sin2\theta+\frac{w}{R}\left[\left(\frac{\pi}{2}+\theta\right)sin^2\theta\right]+18\left(\frac{\pi}{2}+\theta\right)}$$

(2).

Then the effect of dimensionless parameters w/R and arc angle θ on $\varepsilon_{max}/\varepsilon_{app}$ can be obtained as shown by the contour plot in Figure S1b, in which the magnitude of $\varepsilon_{max}/\varepsilon_{app}$ is explained by color scale. Obviously, the effects of the two parameters are all monotonic within the range of interest: the smaller w/R and the larger θ would all contribute to a smaller $\varepsilon_{max}/\varepsilon_{app}$. This is because that smaller w/R represents more slender structures with reduced $\varepsilon_{max}/\varepsilon_{app}$ due to the bending-induced strain whereas larger θ structures could accommodate larger applied strain through enhanced rotational contribution. Apart from only a small region at the lower right corner, the values of $\varepsilon_{max}/\varepsilon_{app}$ are all lower than 1, meaning that adopting the horseshoe-shaped structure of corresponding geometrical parameters is useful in reducing the intrinsic strains of the

material. Considering that large θ would also cause geometric overlap of two neighboring arcs and difficulties in 3D printing process, we adopt $\theta = 42°$. At this fixed arc angle, $\varepsilon_{max}/\varepsilon_{app}$ can be further significantly reduced from 0.39 to 0.02 by decreasing w/R from 1 to 0.1 (denoted by two white dots on the contour plot). The result indicts that changing w/R offers an effective route to alter $\varepsilon_{max}/\varepsilon_{app}$ and the lower limit of w/R is set as 0.1 to study according to the fabrication constrains.

The red dot overlaid on the contour plot with the coordinate (0.17, 42°), which represents the same shape with our FEA models as well as the subsequent printed samples, yields $\varepsilon_{max}/\varepsilon_{app}$ =0.039. This calculated value agrees well with the FEA results of 0.036, validating that the proposed analytical model can accurately predict $\varepsilon_{max}/\varepsilon_{app}$ within the range of interest. The additional line segments in FEA model and small deformation assumption of analytical approach concurrently causes the smaller FEA results than the analytical solution. In conclusion, for a fixed R, stretchability of 3D horseshoe-shaped structures with θ=42° is mainly governed by width w and adopting the narrow design of w=0.17R is expected to improve stretchability by 28 times than its straight counterpart.

REFERENCES

(1) Widlund, T.; Yang, S. X.; Hsu, Y. Y.; Lu, N. S., Stretchability and Compliance of Freestanding Serpentine-Shaped Ribbons. *Int J Solids Struct* **2014,** *51* (23-24), 4026-4037.
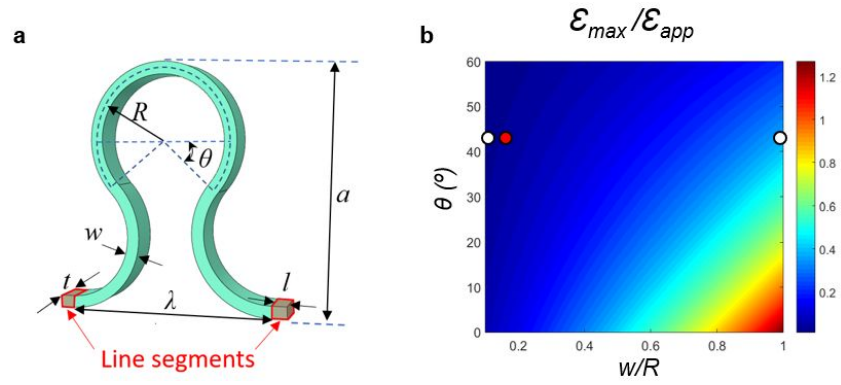
Supplementary Figures

Figure S1. (a). A unit cell of the horseshoe-shaped structure with illustration of the geometrical parameters. (b). Contour plot of $\mathcal{E}_{max}/\mathcal{E}_{app}$ as a function of w/R and arc angle θ of the horseshoe-shaped structure.
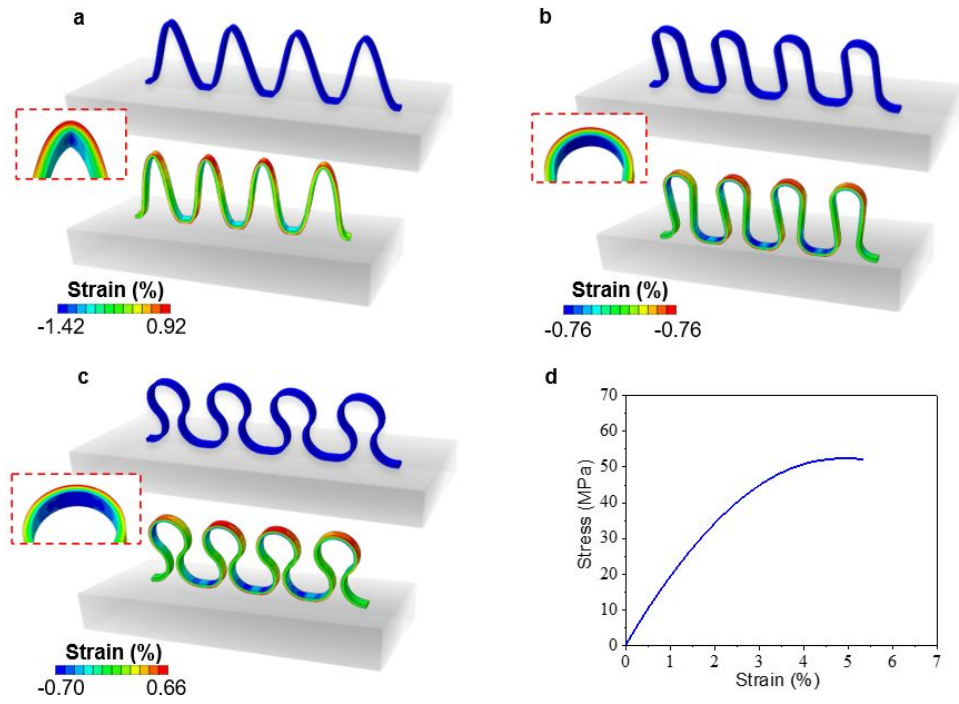
Figure S2. Comparison of max principal strain distribution between (a) sinusoidal structure, (b) U-shaped structure, and (c) horseshoe-shaped structure under 20% compression strain resulted by finite element analyses. The insets correspond to the magnified views of the lower surface of top region. (d). The stress-strain curve of the 3D-printed polymer materials.
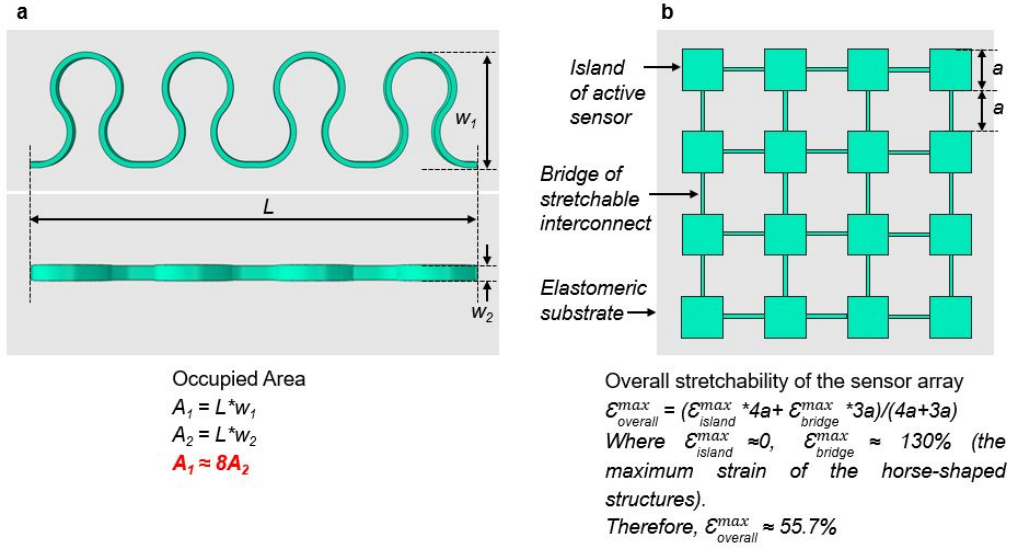
a

w_1

L

w_2

Occupied Area
$A_1 = L*w_1$
$A_2 = L*w_2$
$A_1 \approx 8A_2$

b

Island of active sensor

a

a

Bridge of stretchable interconnect

Elastomeric substrate

Overall stretchability of the sensor array
$\varepsilon_{overall}^{max} = (\varepsilon_{island}^{max} *4a + \varepsilon_{bridge}^{max} *3a)/(4a+3a)$
Where $\varepsilon_{island}^{max} \approx 0$, $\varepsilon_{bridge}^{max} \approx 130\%$ (the maximum strain of the horse-shaped structures).
Therefore, $\varepsilon_{overall}^{max} \approx 55.7\%$

Figure S3. Schematic illustration of (a) comparison of occupied area between 3D and 2D horseshoe-shaped structures, (b) overall stretchability (fracture strain) of the island-bridge design of capacitive pressure sensor arrays.
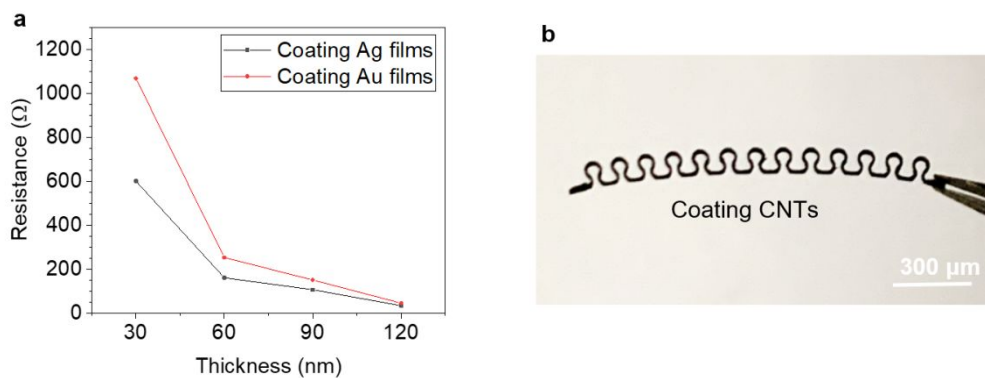
Figure S4. (a). Resistance of 3D horseshoe-shaped microstructure conductor (1cm long, 150 μm wide) coated by Ag or Au films with different thickness. (b). Optical image of 3D horseshoe-shaped microstructures coated by CNTs.
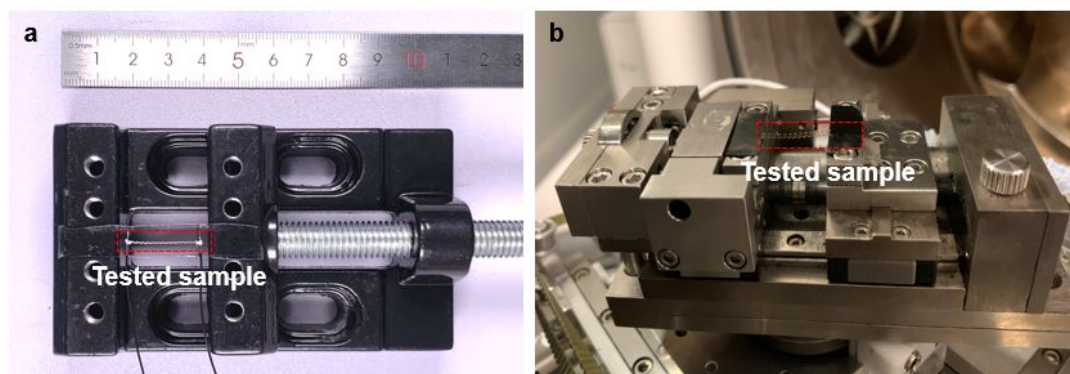
Figure S5. Mechanical testing setups. (a). Customized manual stretcher assisted with a ruler for monotonic tensile test. (b). Microtest mounted on SEM for in-situ tensile test.
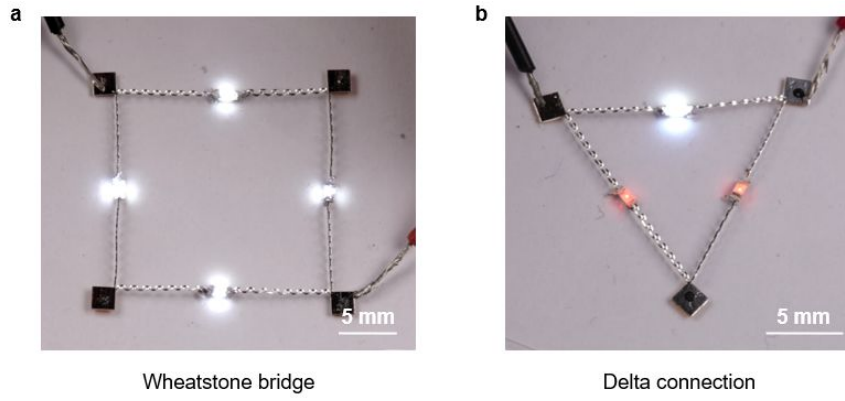
a   Wheatstone bridge   b   Delta connection

Figure S6. Realization of different circuit layouts. (a). Wheatstone bridge. (b). Delta connection.
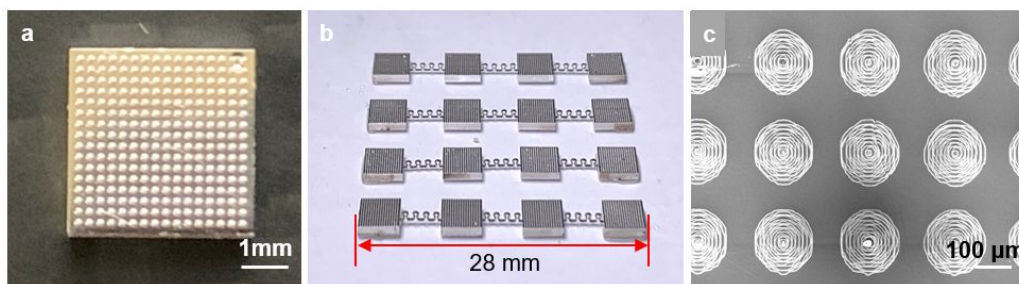
Figure S7. Optical images of (a) a single sensor electrode, and (b) a sensor electrode array, (c) SEM image of surface microstructures of a single sensor electrode from top view.

Supplementary Table

Table S1. Resistance of 3D horseshoe-shaped microstructures coated with different

materials

Coating materials	Resistance (1 cm long, 140 μm wide)
Ag nanowires	50.8 Ω
CNTs	26.3 kΩ
Graphene	12.8 MΩ